

## Sorbates in carbon nanotubes: Transition from diffusive to superdiffusive motion

Shreyas Y. Bhide<sup>1</sup>, Debashree Ghosh<sup>1</sup>, S. Yashonath<sup>1,\*</sup>  
and G. Ananthakrishna<sup>2</sup>

<sup>1</sup>Solid State and Structural Chemistry Unit, and <sup>2</sup>Materials Research Centre, Indian Institute of Science, Bangalore 560 012, India

**Molecular dynamics simulations of sorbates of different sizes confined to the interior of carbon nanotubes are reported. The mean squared displacement shows gradual change from diffusive for small sorbates to superdiffusive for intermediate-sized sorbates to ballistic for sizes comparable to the channel diameter. We show that this crossover behaviour can be understood on the basis of a gradual decrease of the  $x$ - $y$  component of the force with the levitation parameter. We propose that the relevant quantity to understand the recently reported results by others and ourselves, of diffusivities in carbon nanotube is the levitation parameter and not the smoothness of the carbon nanotube. This explanation helps rationalize in a coherent way all of the recently published results.**

CARBON nanotubes are a class of materials which exhibit some remarkable properties that have potential applications<sup>1</sup>. Their nano-sized dimension coupled with closed topology and helicity are known to be responsible for these properties. For instance, the recent findings of Ghosh and co-workers<sup>2</sup> have shown that carbon nanotubes can be used as flow sensors. The elastic modulus of the nanotubes is in the range of 1000 GPa which should find important industrial applications<sup>3</sup>. Recent calculations of self and transport diffusivities in nanotubes show that they are several orders of magnitude larger than those in zeolites<sup>4-9</sup>. A deeper understanding of properties within carbon nanotubes is essential for developing suitable applications.

Unlike zeolites which are aluminosilicates crystallizing in a variety of topologically and geometrically different structures, carbon nanotubes typically take on a cylindrical shape. Single-walled carbon nanotube (SWNT) can be obtained by rolling over a perfect graphene sheet, resulting in tubes with uniform diameter and smooth walls.

Confined fluids often exhibit properties that are quite unlike their bulk counterpart. For example, the self diffusivity,  $D$ , of a sorbate confined within a porous solid is seen to exhibit a maximum as a function of the size of the sorbate, the levitation effect (LE). The dependence of  $D$  on the size of the diffusant,  $\sigma_{\text{gg}}$ , may be divided into two distinct regimes<sup>5</sup>: the anomalous regime occurs when the size of the diffusant,  $\sigma_{\text{gg}}$ , is comparable to the diameter of the pore,  $\sigma_{\text{w}}$  (defined as the distance between the centres

of diagonally opposite carbon atoms) and the commonly observed linear regime, where  $\sigma_{\text{gg}}$  is significantly smaller than the void radius  $\sigma_{\text{w}}$ . In the linear regime  $D \propto 1/\sigma_{\text{gg}}^2$ . The LE is a universal feature seen in all porous solids irrespective of the nature of the pore geometry and topology<sup>6</sup>. A dimensionless levitation parameter  $\gamma$ , characterizing the two regimes, can be defined as the ratio of the distance at which the optimum interaction to the void radius<sup>5</sup> occurs.  $\gamma \sim 1$  in the anomalous regime and much less than unity for the linear regime. In molecular dynamics (MD) simulations with Lennard–Jones (LJ) interaction,  $\gamma = 2^{7/6} \sigma_{\text{gh}}/\sigma_{\text{w}}$ . Here  $\sigma_{\text{gh}}$  and  $\sigma_{\text{w}}$  are the guest–host LJ interaction parameter and void diameter respectively.

There are important differences between porous hosts like zeolites and carbon nanotubes such as smooth walls and uniform diameter. In carbon nanotubes, when the size of the diffusant  $\sigma_{\text{gg}}$  is much smaller than  $\sigma_{\text{w}}$ , the system is three-dimensional. However, as the size of the sorbate approaches that of the void, there is essentially one degree of freedom. It is not clear how these differences will affect the motion within the nanotube. In fact, recent investigations on methane and ethane<sup>7</sup> by us as well as the simulations of H<sub>2</sub> and CH<sub>4</sub> by Skoulidas *et al.*<sup>4</sup>, and Ne and Ar by Ackerman *et al.*<sup>10</sup> corresponding to different effective  $\sigma_{\text{gg}}$  and  $\sigma_{\text{w}}$  reveal that there exists a significant difference in the mobility of these molecules in zeolites compared to carbon nanotubes. In general, the diffusivity within the carbon nanotube is several times that found in zeolites<sup>4,7-10</sup>. Further, it has been shown that the size of the diffusant is one of the important variables that alters the transport properties of sorbates, at least in zeolites<sup>7-9</sup>. This might be important in the case of nanotubes as well. Previous studies have shown that ballistic motion exists for short times (less than 1–2 ps) and this fact has been used to obtain information regarding the nature of the potential energy landscape<sup>11</sup>. But on a longer timescale, studies in zeolites till date have displayed only diffusive behaviour for all sizes of the diffusant. This changes to single file diffusion at high loadings in some one-dimensional zeolites.

Results of detailed MD simulations of spherical sorbates in SWNTs interacting via LJ potential are reported here as a function of the size of the sorbate. We report the transport properties of the sorbates through carbon nanotubes which suggest that the diffusive motion gradually changes over to ballistic motion with increase in  $\sigma_{\text{gg}}$ . More importantly, we show here that this change from diffusive to superdiffusive to eventually ballistic is determined not by the size of the diffusant  $\sigma_{\text{gg}}$  but by the value of the dimensionless levitation parameter  $\gamma$ . Preliminary results have been presented elsewhere<sup>12,13</sup>. Finally, we show that this alone can explain the results obtained by several groups<sup>4,10,14</sup> in the literature.

MD simulations were carried out in the microcanonical ensemble<sup>15</sup> on rigid and flexible carbon nanotubes at 200 K for various sorbate sizes  $\sigma_{\text{gg}} = 1.8, 2.0, 3.0, 7.0 \text{ \AA}$

\*For correspondence. (e-mail: yashonath@sscu.iisc.ernet.in)

in (9, 9) carbon nanotubes of length 49.29 Å and  $\sigma_w = 12.25$  Å.  $N$  (256) and  $N_h$  ( $16 \times 16 \times 720 = 184,320$ ) are the number of sorbates and host atoms at a loading of one sorbate per channel. Equilibration runs were of 2 ns duration and a production run of 20 ns for all sizes except for  $\sigma_{gg} = 7.0$  Å where the run length is 100 ns. The potential of Hummer *et al.*<sup>16</sup> has been used for flexible nanotube simulations.

MD simulations of rigid carbon nanotubes have been carried out using the velocity Verlet algorithm<sup>8</sup> at 200 K for various sorbate sizes,  $\sigma_{gg} = 1.8, 2.0, 3.0, 7.0$  Å with mass 39.95 amu. A  $16 \times 16$  array of (9, 9) carbon nanotubes (armchair-type) of length 49.29 Å and  $\sigma_w = 12.25$  Å with centres of two tubes separated by 15.65 Å, were placed on a triangular lattice. The LJ (6–12) interaction  $\phi(r) = 4 \epsilon [(\sigma/r)^{12} - (\sigma/r)^6]$  is used for sorbate and host atoms. The total potential energy of the system is

$$U = \sum_{i \neq j}^N \phi_{ij}^{gg}(r) + \sum_{i=1}^N \sum_{j=1}^{N_h} \phi_{ij}^{gh}(r_{ij}), \quad (1)$$

where  $N$  (256) and  $N_h$  ( $16 \times 16 \times 720 = 184,320$ ) are the number of sorbates and host atoms. The interactions are modelled with  $\epsilon_{gg} = 0.9975$  kJ/mol (119.8 K),  $\sigma_{hh} = 3.4$  Å and  $\epsilon_{hh} = 0.2328$  kJ/mol (38 K). Except for  $\sigma_{gg} = 1.8$  Å, Lorentz–Berthelot rule was used for guest–host interactions (Table 1). Periodic boundary conditions are applied along the tube axis (z-axis). A cut-off radius of 15 Å has been employed. One sorbate is placed in each of the nanotubes. The integration time step of 10 fs is used with equilibration for 2 ns and a production run of 20 ns, in particular 100 ns for  $\sigma_{gg} = 7.0$  Å. Calculations have also been carried out at a higher loading of three sorbates per channel length of 49.29 Å for  $\sigma_{gg} = 7$  Å. This corresponds to 12 sorbates for every four channels or about 44% of saturation loading which may be compared to the low loading of 4 per unit cell at which most of the calculations reported here have been performed.

Flexible nanotube calculations have been carried out using the model of Hummer *et al.*<sup>16</sup> at a temperature of 400 K for guest size of  $\sigma_{gg} = 7.0$  Å. Other details of the calculations are the same as those used for rigid nanotubes.

Figure 1 shows a log–log plot of mean square displacement (MSD) of the sorbates (averaged over 256 particles and MD trajectories) for different  $\sigma_{gg}$  values. The MSDs are shown over three orders of magnitude, approximately for the period 10–1000 ps. The MSDs can be fitted to

**Table 1.** Exponent values of  $\alpha$  calculated from rigid nanotube MD simulations

$\sigma_{gg}$ (Å)	$\sigma_{gh}$ (Å)	$\gamma$	$\alpha_{MD}$
1.8	1.8	0.32	0.95
2.0	2.7	0.49	1.30
3.0	3.2	0.59	1.64
7.0	5.2	0.95	1.94

$u^2(t) \sim t^\alpha$ . The exponent values have been evaluated using the MSD data in the range 100–1000 ps, where the statistics is good. The transport is essentially diffusive for the smallest size,  $\sigma_{gg} = 1.8$  Å with  $\alpha = 1.03$ . Note that the motion is ballistic at short times for small  $\sigma_{gg}$ , as it should be. Table 1 shows that  $\alpha$  increases from 1 to 2 with size, indicating that the extent of the ballistic transport increases with size and eventually the sorbate behaves like a free particle<sup>17</sup>. Further, flexible carbon nanotube simulations at the same temperature were also carried out and the trend seen in Table 1 remains unchanged, with a marginal decrease in the exponent value<sup>17</sup>.

Previous studies to date by Skoulidas *et al.*<sup>4</sup>, Ackerman *et al.*<sup>10</sup> and Sokhan *et al.*<sup>14</sup> have reported self-diffusivity values in carbon nanotubes. These authors did not find the presence of superdiffusive motion within carbon nanotubes. In contrast, studies by Bhide *et al.*<sup>7–9</sup> have reported the presence of motion which shows that the MSD varies nonlinearly ( $u^2(t) \sim t^\alpha$ ) with time within carbon nanotubes.

A careful study of the nature of the trajectories for various sizes of sorbates gives useful insight into the changes in the dynamics, as reflected in the increasing superdiffusive behaviour.

A projection onto the  $xy$ -plane is shown in Figure 2, for various sizes and initial conditions. It is clear that the sorbate motion predominantly covers the whole volume within the nanotube (Figure 2a) when the sorbate diameter is small, e.g.  $\sigma_{gg} = 1.8$  Å. With increase in size, they are confined to the vicinity of the walls of the nanotube (Figure 2b for  $\sigma_{gg} = 3.0$  Å). The motion is largely random or chaotic in both these cases. This is evident when the trajectory is projected onto the  $xy$ -plane. The sorbate motion gradually is restricted to an annular region of increasingly smaller radius close to the channel axis, with further increase in size. Figure 2c and d shows such trajectories on an expanded scale for size  $\sigma_{gg} = 7$  Å. Note that the motion is less random or more regular. This behaviour is seen when the size of particle is comparable to that of the free diameter of the nanotube (i.e.  $\gamma = 0.95$ , corresponding to the anomalous regime of the LE). The

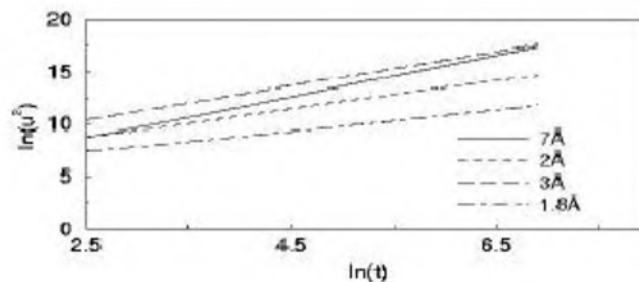


**Figure 1.** Log–log plot of  $u^2(t)$  vs  $t$  for 1 ns duration varying over three orders of magnitude for different sizes of sorbates calculated from MD.  $\sigma_{gg} = 1.8, 2.0, 3.0, 7.0$  Å. The time is in units of ps and MSD in Å<sup>2</sup>.

trajectory is nearly one-dimensional for this size. The motion (unlike that seen in Figure 2 *a*) is highly regular. In general, for  $\sigma_{gg} = 7.0 \text{ \AA}$ , we found that the geometrical structure of the trajectories is sensitive to the initial conditions illustrated for two sets in Figure 2 *c* and *d*. Figure 2 *c* displays a fan-like structure with dominant streaks similar to those seen in the Poincaré maps of Hamiltonian systems. However, we stress that the MSDs obtained here are averages over various initial conditions provided by different particles. Also, note that the sorbate particles interact with each other since the cut-off radius is  $15 \text{ \AA}$ ; although two nanotube centers are separated by  $15.65 \text{ \AA}$ , two sorbates placed in neighbouring nanotubes can come as close as  $15.65 - 12.25 = 3.4 \text{ \AA}$  of each other. Therefore, the simulations reported here do not correspond to isolated, non-interacting sorbates. For  $\sigma_{gg} = 7.0 \text{ \AA}$ , for which  $\alpha = 1.94$  for the 20 ns run, we carried out a 100 ns ( $0.1 \mu\text{s}$ ) long run to verify that these results remain unchanged. The value of the exponent  $\alpha$  from the 100 ns run is 1.975, slightly higher than that obtained from the 20 ns run. This clearly suggests that the 20 ns run lengths are adequate. We also carried out calculations for 3 guests/channel for  $\sigma_{gg} = 7 \text{ \AA}$  and found that the superdiffusive motion persists with a marginally lower value of  $\alpha = 1.90$ .

The dynamics of the sorbate is essentially determined by the force experienced by the sorbate due to the field of nanotube atoms. In order to gain additional insight into the reasons for the crossover from diffusive to ballistic transport, we calculate the mean squared force,  $\langle F_z^2 \rangle$ , experienced by the sorbate molecule as a function of  $\gamma$ . (Here  $\langle \dots \rangle$  refers to the time average.) The decreasing

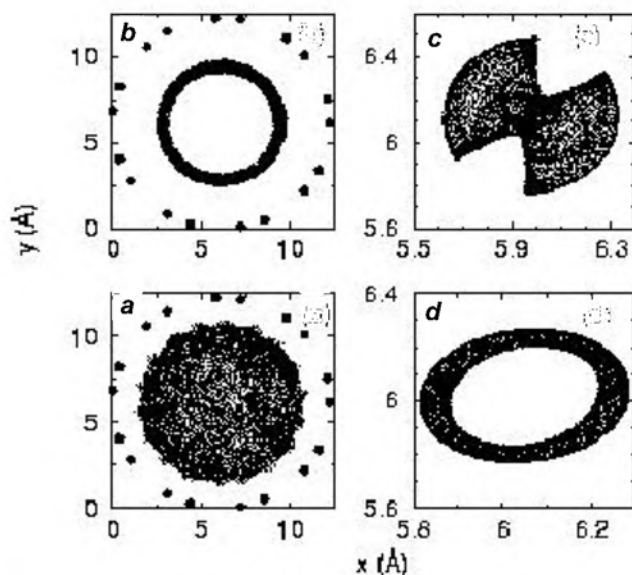


**Figure 2.** Projections of various types of trajectories for various  $\sigma_{gg}$  onto the  $xy$ -plane. *a*,  $\sigma_{gg} = 1.8 \text{ \AA}$ ; *b*,  $\sigma_{gg} = 3.0 \text{ \AA}$ . Black outer dots represent atoms of carbon nanotube. *c*, *d*, Fan and ring-like structures on an expanded scale for  $\sigma_{gg} = 7.0 \text{ \AA}$  for two different initial conditions.

nature of  $\langle F_z^2 \rangle$  with  $\gamma$  signals the change in the nature of the dynamics from a diffusive to superdiffusive nature, i.e.  $\langle F_z^2 \rangle \rightarrow 0$  as  $\gamma \rightarrow 1$  with increasing size ( $\sigma_{gg}$  approaching the free diameter of the nanotube), underscoring the cause of the ballistic motion for  $\sigma_{gg} = 7.0 \text{ \AA}$  (Figure 3). This should be contrasted with the results obtained in other microporous solids such as zeolites. In zeolites like NaY, NaA or VPI-5, the mean squared force shows a minimum<sup>5</sup> when  $\gamma \approx 1$ . However, we note that the net force even when it is minimum remains significant in the case of zeolites. In contrast, in case of the nanotube, the force becomes quite insignificant at the largest size. The reason for this is that zeolites have a nonuniform diameter throughout. Thus, though  $\langle F_z^2 \rangle$  is smaller for particles of size similar to that of the pore or window, force cancellation occurs only at the window connecting the cages. In contrast, as carbon nanotubes have uniform pore diameter and smooth walls, the frictional force experienced by the sorbate nearly vanishes everywhere along the tube for large  $\sigma_{gg}$ , rendering the motion superdiffusive.

Does superdiffusive motion persist at higher loadings? We have carried out simulations at 3 sorbates/channel for the largest size,  $\sigma_{gg} = 7.0 \text{ \AA}$ . The time evolution of the mean squared displacement is seen in Figure 4. It is evident

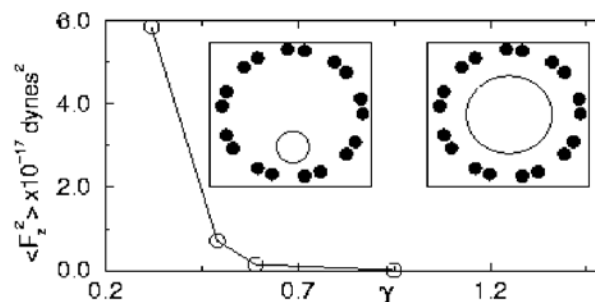


**Figure 3.** Mean squared force along the nanotube obtained from MD versus levitation parameter  $\gamma$ . (Inset) Schematic diagrams for a small and large-sized sorbate in the nanotube.

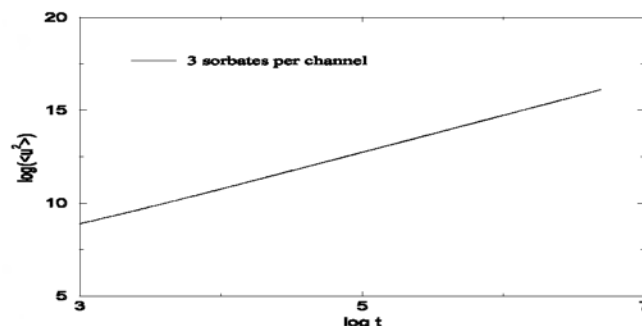


**Figure 4.** Time evolution of mean squared displacement for  $\sigma_{gg} = 7.0 \text{ \AA}$  for a higher loading of three sorbates/channel. This corresponds to 44% of the saturation loading, thus showing that superdiffusive motion persists even at higher loadings. The exponent  $\alpha$  decreases from 1.97 at 1 sorbate/channel to 1.90 at 3 sorbates/channel.

that even at this high loading of approximately 44% of the saturation loading, the exponent  $\alpha$  remains superdiffusive. The value of  $\alpha$  is 1.90 compared to 1.975 for 1 sorbate/channel. Further, the work of Skoulidas *et al.*<sup>4</sup> and Ackerman *et al.*<sup>10</sup> suggests that the transport diffusivity is not a decreasing function of loading. These results show that it might be possible to exploit the superdiffusive motion for technological gains.

As we shall show, our approach based on the levitation parameter helps us to understand the totality of the results on diffusivities of guests in carbon nanotubes reported recently<sup>4,10</sup>. In a recent simulation, Skoulidas *et al.*<sup>4</sup> report self- and transport diffusivities of H<sub>2</sub> and CH<sub>4</sub>. They find that the self- and transport diffusivities of H<sub>2</sub> are higher in the narrower (6, 6) nanotube compared to the (10, 10) nanotube by about a factor of 4 and 10 respectively. Sholl and co-workers suggest that this can be explained based on the increasing smoothness<sup>4,10</sup> of narrower tubes. They suggest that, 'The higher curvature of the (6, 6) nanotube leads to a smoother potential energy surface (PES) for H<sub>2</sub>-wall than for (10, 10) SWNT'. As we shall argue, this qualitative reasoning is not adequate to explain the totality of the results on Ne and Ar, while it appears to explain the results on H<sub>2</sub>. In fact, Ackerman *et al.*<sup>10</sup> report that  $D$  for Ne is lowest for (8, 8) followed by (10, 10) and then by (12, 12). In other words,  $D(8, 8) < D(10, 10) < D(12, 12)$  for Ne, which is inverse of the behaviour found for H<sub>2</sub>. More interesting is the non-monotonic change in  $D$  for Ar, namely,  $D(8, 8) > D(10, 10) < D(12, 12)$ . The values of self diffusivities obtained from Skoulidas *et al.*<sup>4</sup> and Ackerman *et al.*<sup>10</sup> are listed in Table 2.

We offer here an alternative explanation based on levitation effect<sup>5</sup> which provides a quantitative measure as well. As already pointed out, the variation of self-diffusivity with size is non-monotonous. Initially, in the linear regime, the self-diffusivity,  $D \propto 1/\sigma_{\text{gg}}^2$ , where  $D$  decreases with increase in size of the sorbate or diffusant. But as the size of the diffusant approaches that of the void,  $D$  exhibits a maximum resulting in an  $N$ -shaped curve. In terms of  $\gamma$ ,  $D$  decreases with increasing  $\gamma$  initially, but later increases leading to a maximum and finally decreases with  $\gamma$ . (See figure 9 in Yashonath and Santikary<sup>5</sup>). Now consider the results of Sholl and co-

workers<sup>4,10</sup>, who have studied diffusion within carbon nanotubes of differing diameters. To understand their results, we use the dimensionless levitation parameter,  $\gamma$ , defined as the ratio of the distance at which optimum interaction occurs to the void radius that is the relevant quantity. In order to explain their results, we need the potential parameters used by Sholl and co-workers<sup>4,10</sup>, who do not provide them, making it difficult to compute the value of  $\gamma$ . However, we have obtained the potential parameters from the references cited by Sholl and co-workers<sup>4,10</sup>. The values we compute are therefore approximate, but are adequate to explain the trends shown in Table 2. An estimate of  $\gamma$  for H<sub>2</sub> in (6, 6) nanotube is approximately 0.78 compared to relatively small value of  $\sim 0.47$  in (10, 10) nanotube. Further, from Figure 3, it is evident that  $\langle F_z^2 \rangle$  is close to zero for  $\gamma = 0.78$  and hence lies in the anomalous regime, consequently a higher diffusivity in the (6, 6) nanotube. In contrast, for  $\gamma = 0.47$ ,  $\langle F_z^2 \rangle$  is substantial and thus  $D$  for (10, 10) is lower. (Note that  $\gamma$  is to a large extent independent of the system as it is the ratio of the optimum interaction distance to the pore size).

We now consider the variation of  $D$  for Ne in the three carbon nanotubes. Ackerman *et al.*<sup>10</sup> report that  $D$  for Ne is lowest for (8, 8) followed by (10, 10) and then by (12, 12), i.e.  $D(8, 8) < D(10, 10) \leq D(12, 12)$ . If we invoke the simple-minded smoothness explanation offered by Sholl and co-workers<sup>4,10</sup>, then  $D$  should have precisely the reverse trend, i.e.  $D(8, 8) > D(10, 10) > D(12, 12)$ , as the smoothness of the (8, 8) carbon nanotube is higher than the smoothness of (12, 12) carbon nanotube! However, from our perspective, the value of  $\gamma$  for (8, 8) is 0.56, for (10, 10) 0.45 and for (12, 12) 0.38. From Yashonath and Santikary<sup>5</sup>, who report the dependence of self-diffusivity on  $\gamma$ , we know that the linear regime (where a monotonic dependence of  $D$  on size is seen) exists for small values of  $\gamma$ . The range of  $\gamma$  values for Ne (0.38–0.56) in the three carbon nanotubes all appear to lie in the linear regime. This clearly leads to a monotonic decreasing dependence of  $D$  on  $\gamma$ , thus explaining the results of Ackerman *et al.*<sup>10</sup>.

A more interesting situation is the non-monotonic change in  $D$  for Ar, namely  $D(8, 8) > D(10, 10) < D(12, 12)$ . Skoulidas *et al.*<sup>4</sup> as well as Ackerman *et al.*<sup>10</sup> report error bars which are small and therefore these trends in the values of  $D$  for Ne, Ar (see below) as well as those of H<sub>2</sub> in various carbon nanotubes are unambiguous. Clearly, the smoothness explanation of Sholl and co-workers fails here as in the case of Ne. However, this result can be understood from the non-monotonic dependence of  $D$  on  $\sigma_{\text{gg}}$ . As stated earlier, a non-monotonic dependence can arise when the values of the parameter  $\gamma$  fall in two distinct situations, namely (i) anomalous regime alone and (ii) transition from the linear to the anomalous regime. Our estimates of  $\gamma$  for Ar in  $(n, n)$ ,  $n = 8, 10, 12$  nanotubes are: 0.63 for (8, 8) nanotube, 0.50 in (10, 10) and

**Table 2.** Self-diffusivities at highest loading and room temperature for various guests (represented by a single interaction site and spherical sorbates, interacting via LJ potential) in carbon nanotubes of differing diameters<sup>4,10</sup>

Guest	Carbon nanotube			
	(6, 6)	(8, 8)	(10, 10)	(12, 12)
H <sub>2</sub>	$2 \times 10^{-2}$		$2 \times 10^{-3}$	
Ne		$1 \times 10^{-3}$	$2 \times 10^{-3}$	$2.1 \times 10^{-3}$
Ar		$4 \times 10^{-4}$	$2 \times 10^{-4}$	$4 \times 10^{-4}$

0.42 in (12, 12). The values of  $\gamma$  obtained here suggest it is likely to be situation (ii), namely the transition from linear to the anomalous regime. The larger value of  $\gamma = 0.63$  for Ar in (8, 8) might mean that it lies in the anomalous regime where  $D$  increases with  $\gamma$ . On the other hand, the values 0.50 and 0.42 in all likelihood lie in the linear regime. The value of  $\gamma = 0.50$  most likely corresponds to the minimum in  $D$  at the transition from linear to the anomalous regime. Thus our inference is that in the case of Ar,  $\gamma$  lies in the crossover from the linear to the anomalous regime and therefore has a non-monotonic dependence. Thus, a more convincing explanation of the self-diffusivity and its variation in nanotubes of different diameters suggest that smoothness cannot explain the trends seen, although smoothness might offer a suitable explanation for the higher diffusivities of guests in carbon nanotubes compared to zeolites.

In summary, our study demonstrates a crossover from a diffusive behaviour (with  $\alpha \approx 1$ ) at small sizes ( $\gamma < 0.5$ ) of the sorbate to superdiffusive nature ( $1 < \alpha < 2$ ) with increase in size, eventually approaching ballistic motion when the sorbate size is similar to that of the host. The crossover has been explained quantitatively:  $\langle F_z^2 \rangle$  decreases with increase in the levitation parameter  $\gamma$  (eventually vanishing as  $\gamma \rightarrow 1$ ; Figure 3). The superdiffusive nature is not suppressed even at higher loadings (at least up to 44% of saturation loading). Temperature variation suggested the temperature dependence of the diffusion constant to be non-Arrhenius. Flexible nanotube simulations for  $\sigma_{\text{gg}} = 7 \text{ \AA}$  at the same temperature yield marginally lower exponent. Indeed, even at a relatively higher temperature of 400 K, we found<sup>17</sup>  $\alpha = 1.68$ . More detailed simulations to understand the contributions from different factors to the observed behaviour are in progress. Finally, the line of reasoning based on the levitation parameter affords a basis for explaining the seemingly conflicting trends of Skoulidas *et al.*<sup>4</sup> and Ackerman *et al.*<sup>10</sup>.

12. Bhide, S. Y., Debashree Ghosh, Yashonath, S. and Ananthakrishna, G., *StatPhysics*, (Abstr.) 2004, **22**, 282.
13. Bhide, S. Y., Debashree Ghosh, Yashonath, S. and Ananthakrishna, G., 2004, *cond-mat/0407723*.
14. Sokhan, *et al.*, *J. Chem. Phys.*, 2002, **117**, 8531; 2001, **115**, 3878.
15. Allen, M. P. and Tildesley, D., *Computer Simulation of Liquids*, Clarendon Press, Oxford, 1986.
16. Hummer, G., Rasaiah, J. C. and Noworyta, J. P., *Nature*, 2001, **414**, 188.
17. Bhide, S. Y., Diffusion of polyatomic and monatomic sorbates in zeolites and microporous solids: Molecular dynamics and lattice gas studies. Ph D thesis, submitted to Indian Institute of Science, Bangalore, December 2002.

ACKNOWLEDGEMENT. We thank DST, New Delhi for financial support.

Received 28 July 2004; revised accepted 17 August 2004

1. Ajayan, P. M., *Chem. Rev.*, 1999, **99**, 1787.
2. Ghosh, S., Sood, A. K. and Kumar, N., *Science*, 2003, **299**, 1042–1044; Cohen, A. E., Ghosh, S., Sood, A. K. and Kumar, N., *Science*, 2003, **300**, 1235.
3. Yu, M. F. *et al.*, *Phys. Rev. Lett.*, 2000, **84**, 5552; *Tans.*, S. J. *et al.*, *Nature*, 1997, **386**, 474.
4. Skoulidas, *et al.*, *Phys. Rev. Lett.*, 2002, **89**, 185901.
5. Yashonath, S. and Santikary, P., *J. Phys. Chem.* 1994, **98**, 6368.
6. Bandyopadhyay, S. and Yashonath, S., *J. Phys. Chem.*, 1995, **99**, 4286.
7. Bhide, S. Y. and Yashonath, S., *J. Chem. Phys.*, 2002, **116**, 2175.
8. Bhide, S. Y. and Yashonath, S., *J. Phys. Chem. A*, 2002, **106**, 7130; Bhide, S. Y. and Yashonath, S., *J. Phys. Chem. B*, 2000, **104**, 11977.
9. Bhide, S. Y. and Yashonath, S., *J. Am. Chem. Soc.*, 2003, **125**, 7425.
10. Ackerman, D. M. *et al.*, *Mol. Simul.* 2003, **29**, 677.
11. Ghosh, M., Ananthakrishna, G., Yashonath, S., Demontis, P. and Suffritti, G., *J. Phys. Chem.*, 1994, **98**, 9354.